EcoHealth 19, 458–462, 2022
https://doi.org/10.1007/s10393-022-01623-6

EcoHealth

Short Communication

A Novel Host of an Emerging Disease: SARS-CoV-2 Infection in a Giant Anteater (*Myrmecophaga tridactyla*) Kept Under Clinical Care in Brazil

Asheley Henrique Barbosa Pereira,[1] Gabriela Oliveira Pereira,[1] Jaqueline Camargo Borges,[2] Victoria Luiza de Barros Silva,[3] Bárbara Hawanna Marques Pereira,[4] Thays Oliveira Morgado,[4] Joao Paulo da Silva Cavasani,[5] Renata Dezengrini Slhessarenko,[6] Richard Pacheco Campos,[3] Alexander Welker Biondo,[7] Renan de Carvalho Mendes,[8] Pedro Eduardo Brandini Néspoli,[8] Marcos Almeida de Souza,[5] Edson Moleta Colodel,[5] Daniel Guimarães Ubiali,[1] Valéria Dutra,[2] and Luciano Nakazato[2]

[1]*Setor de Anatomia Patológica (SAP), Universidade Federal Rural do Rio de Janeiro (UFRuralRJ), BR-465 Km7, Seropédica, Rio de Janeiro, Brasil*
[2]*Laboratório de Microbiologia e Biologia Molecular Veterinária, UFMT, Av. Fernando Corrêa da Costa 2367, Bairro Boa Esperança, Cuiabá, Mato Grosso, Brasil*
[3]*Laboratório de Parasitologia Veterinária e Doenças Parasitárias dos Animais Domésticos e Silvestres, UFMT, Av. Fernando Corrêa da Costa 2367, Bairro Boa Esperança, Cuiabá, Mato Grosso, Brasil*
[4]*Setor de Animais Silvestres, Hospital Veterinário, UFMT, Av. Fernando Corrêa da Costa 2367, Bairro Boa Esperança, Cuiabá, Mato Grosso, Brasil*
[5]*Laboratório de Patologia Veterinária, UFMT, Av. Fernando Corrêa da Costa 2367, Bairro Boa Esperança, Cuiabá, Mato Grosso, Brasil*
[6]*Hospital Universitário Júlio Muller, UFMT, Av. Fernando Corrêa da Costa 2367, Bairro Boa Esperança, Cuiabá, Mato Grosso, Brasil*
[7]*Departamento de Medicina Veterinária, Universidade Federal do Paraná, Curitiba, Paraná, Brasil*
[8]*Faculdade de Medicina Veterinária, UFMT, Av. Fernando Corrêa da Costa 2367, Bairro Boa Esperança, Cuiabá, Mato Grosso, Brasil*

Abstract: A young male free-ranging giant anteater (*Myrmecophaga tridactyla*) was found with paralysis of pelvic limbs on a highway and kept under human care. Radiographs confirmed multiple incomplete fractures in the thoracolumbar vertebrae. Due to the poor prognosis, euthanasia was chosen. The infection was established by viral SARS-CoV-2 RNA detection in the rectal swab, spleen and kidney samples. Immunohistochemistry detected the viral nucleocapsid protein in sections of the lungs, liver, spleen, lymph nodes, and large intestine sections, and spike protein antigen in the lung tissue. Pilosa order species should be included as potential hosts of natural infection of SARS-CoV-2.

Keywords: Spillover, Spillback, Pilosa order, Immunohistochemistry, SARS-CoV-2, COVID-19

The giant anteater (*Myrmecophaga tridactyla*, Pilosa: Myrmecophagidae) is a vulnerable, endangered species. In Brazil, it is considered possibly extinct in Rio de Janeiro, Espírito Santo, Santa Catarina, Rio Grande do Sul states and in a significant risk of disappearance in Central America (Miranda et al. 2014). The emergence of a pathogen to a distinct species offers a potential threat to conservation.

Published online: January 24, 2023

Correspondence to: Luciano Nakazato, e-mail: lucnaka@gmail.com

Severe Acute Respiratory Syndrome Coronavirus 2 (SARS-CoV-2), a recently emerged coronavirus species, is responsible for an ongoing worldwide pandemic of a disease identified as coronavirus disease 2019 (COVID-19) (Johnston et al. 2021). Widespread human SARS-CoV-2 infections combined with human-wildlife interactions create the potential for reverse zoonosis from humans to wildlife (Chandler et al. 2021).

A free-ranging 10.6 kg young male giant anteater (*Myrmecophaga tridactyla*) was found without previous clinical history on a highway in Cuiabá, Mato Grosso State, Brazil, on January 7th, 2022. The giant anteater was referred to a private veterinary clinic 3 days after the rescue. The first physical evaluation of the giant anteater revealed paralysis of pelvic limbs, apathy, moderate pale mucous membranes, and abdominal distension. Intense clinical care was established with chloramphenicol (15 mg/kg IM SID during 7 days), dexamethasone (1 mg/kg SC SID during 5 days), and vitamin K (15 mg/kg IM SID during 7 days). Supportive treatment consisted of intensive intravenous glucose therapy fluid. On January 15th, 2022, the dose of dexamethasone was halved.

On January 18th, 2022, the *M. tridactyla* was submitted to a radiograph, and multiple incomplete fractures were seen in the thoracolumbar vertebrae. The chest radiograph revealed all pulmonary lobes with mild radiopacity increase and diffuse bronchointerstitial pattern. Due to the poor prognosis, euthanasia was chosen, and the carcass was submitted for necropsy. All procedures were conducted in full compliance and approval by the Brazilian Ministry of the Environment (SISBIO 79,317–1).

A complete necropsy was performed, and fragments of the lung, brain, spinal cord, heart, kidney, urinary bladder, spleen, liver, stomach, and small and large intestines were sampled and fixed by immersion in 10% neutral buffered formalin. The fixed tissues were processed conventionally, embedded in wax, cut at 3 microns, stained with hematoxylin and eosin, and examined by optical microscope.

Grossly, body score 3 (1 to 5 scale) was observed. There was a focally extensive amorphous red fluid in the epidural space on the spinal canal, from the lumbar to the cervical region. Extending from the carina region to the cervical portion, the tracheal lumen was filled with a large amount of white mucous fluid. In the lungs, there was mild edema in the interlobar septa. The lung lobes were diffusely and slightly enlarged and showed multifocal to coalescent red and irregular, firm, and poorly demarked dark red areas [Fig. 1A]. There were approximately 100 ml of translucent yellowish fluid in the abdominal cavity. The mesenteric and intestinal vessels showed evident congestion. The gastric mucosa was diffused and slightly red with multifocal areas with several adhered nematodes.

The gastrointestinal content was sampled at necropsy and forwarded to the Laboratory of Parasitology and Parasitic Diseases of Domestic and Wild Animals. The gastrointestinal contents were washed in running water, sieved with a metallic mesh of 100 μm, placed in glass vials, and observed under a stereoscopic microscope to collect helminths. All recovered helminths were either clarified or partially conditioned in 70% alcohol. These nematodes exhibited two large, simple, triangular lateral lips, each apically provided with teeth and externally with papillae. The cuticle was folded over the lips with a short buccal cavity. In males, it was possible to visualize long caudal wings, while females had the vulva in the middle of the posterior part of the body. The egg is visualized as thick-shelled and embryonated. According to Anderson et al. (2009); Vicente et al. (1997), and Ortlepp (1922), these nematodes were classified into the genus *Phylasoptera* sp.

At the lung histological evaluation, the alveolar septa were multifocally expanded through examination by a mild proliferation of alveolar macrophages, and perivascular lymphohistiocytic infiltrate [Fig. 1B]. Diffusely there was a mild alveolar macrophage proliferation that often exhibited abundant and foamy cytoplasm. Multifocally, discreet hypertrophy of type 1 pneumocytes and proliferation of type 2 pneumocytes were observed. A hyaline amorphous material filled the alveolar lumen in these areas. Many erythrocytes diffusely distended the pulmonary blood vessels, and occasional hemosiderophages were noted in the alveolar septa.

A severe multifocal to coalescent, chronic ulcerative gastritis associated with nematodes was found. In the small intestine, multifocal and mild fibrous thickening was observed in the lamina propria and submucosa. Related to these areas, multiple nematodes were visualized. The lumbar spinal cord sections revealed white matter diffuse and moderately vacuolated with several digestion chambers. There were numerous axonal spheroids, often in ventral funiculi. Central chromatolysis was noted in the neuronal bodies. No histological changes were observed in the brain, kidney, urinary bladder, spleen, and large intestine sections.

Immunohistochemistry (IHC) anti-SARS-CoV Nucleocapsid Protein (NP) was employed in the lung, heart, kidney, spleen, liver, stomach, small and large intestines, and spinal cord sections, according to Jarrah et al. (2022),

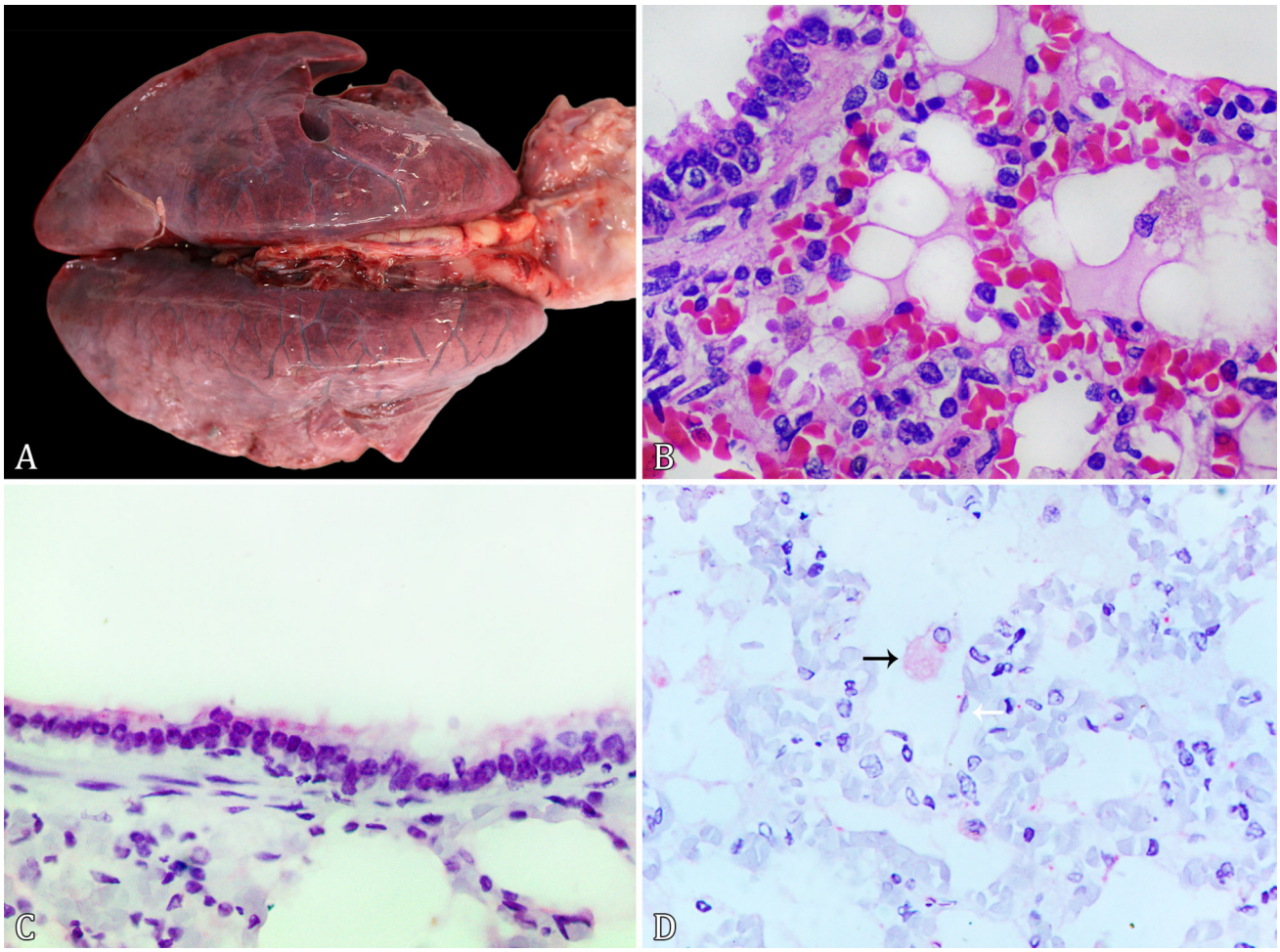

Figure 1. Pathological and immunohistochemical findings of SARS-CoV-2 natural infection in a free-ranging giant anteater (*Myrmecophaga tridactyla*) kept under human clinical care. **A** The lung lobes show multifocal to coalescent red and irregular, firm, and poorly demarked red to dark areas. **B** The alveolar septa were expanded by a mild lymphohistiocytic infiltrate. A hyaline amorphous material filled the alveolar lumen in these areas (HE, Obj. 40×). **C** Strong cytoplasmic immunolabeling in the respiratory epithelium of bronchiole (IHC, anti-nucleocapsid protein. Obj. 40×). **D** Moderate cytoplasmic immunolabeling in alveolar macrophages (black arrow) and mild cytoplasmic immunolabeling in type 1 pneumocyte (white arrow) (IHC, anti-spike protein. Obj. 40×).

with minor modifications. Additional IHC using anti-SARS-CoV-2 spike protein (S) was employed in the lung sections according to Pereira et al. (2022). Both NP and S antibodies were employed as the same protocols in the lungs of a giant anteater that died before the global emergence of SARS-CoV-2. In these additional control cases, no immunolabeling against both antibodies was observed.

The IHC anti-NP revealed multifocal, strong cytoplasmic immunolabeling in the respiratory epithelium of bronchi and bronchioles [Fig. 1C], and in type 1 and 2 pneumocytes. Large numbers of macrophages in alveoli and alveolar septa exhibited strong granular cytoplasmic immunolabeling. Multifocally, intense immunolabeling was observed delineating the wall of the alveolar septa. Numerous macrophages with cytoplasmic immunolabeling were observed in spleen sections. Intestinal glands of the large intestine expressed strong cytoplasmic immunolabeling. No anti-SARS-CoV nucleocapsid protein immunoexpression was observed in the heart, liver, kidney, urinary bladder, jejunum and spinal cord sections. Immunohistochemistry against SARS-CoV-2 spike protein in the lungs showed multifocal, moderate cytoplasmic immunolabeling in macrophages in the alveolar lumen and alveolar septa and rarely in the type 1 and 2 pneumocytes [Fig. 1D].

The *M. tridactyla* reported herein showed mild interstitial lymphohistiocytic pneumonia and no diffuse alveolar damage (DAD). To date, no animal model has consistently

exhibited DAD following inoculation with SARS-CoV-2 (Johnston et al. 2021). We attributed the severe lumbar spinal cord demyelination to trauma in the thoracolumbar vertebrae. Our IHC results are compatible with previous experimental studies in biomodels like rhesus monkeys (Munster et al. 2020), which describe viral nucleocapsid antigen detection in pulmonary, gastrointestinal and lymphoid tissues. The IHC can be an ancillary tool for SARS-CoV-2 diagnosis.

Angiotensin-converting enzyme 2 (ACE2) receptor was surveyed by IHC in sections of the lung, small intestine, large intestine, urinary bladder, liver, heart, spleen and spinal cord, according to Lean et al. (2021), with minor modifications. The ACE2 receptor was detected with moderate immunolabeling on the brush border of the apical surface of small intestine enterocytes and epithelial cells of the proximal convoluted tubules of the kidney. Immunoexpression of ACE2 receptor was negative in the lung, heart, liver, spleen, urinary bladder, stomach, large intestine and spinal cord sections.

A study predicted that the ACE2 proteins of giant anteater were classified as having a high propensity for binding the SARS-CoV-2 receptor binding domain of spike protein; thus, they are potentially susceptible hosts to infection (Damas et al. 2020). To the author's knowledge, ACE2 expression in the giant anteater tissues was not demonstrated previously. The SARS-CoV-2 NP and S antigen in several giant anteater tissues suggests that this host can be infected even with the absence of pulmonary detection of ACE2 by IHC. Similar findings were described in a highly susceptible species to SARS-CoV-2 infection, the Syrian hamster (*Mesocricetus auratus*) (Lean et al. 2021). Even with results of IHC anti- SARS-CoV-2 NP strongly immunolabeled in epithelial cells of intestinal glands and ACE2 receptor detection in enterocytes, we cannot determine the exact route of SARS-CoV-2 natural infection in this giant anteater, and further studies need to clarify this pathogenesis.

Swabs of the nasopharynx, oropharynx and rectum and fragments of multiple organs were sampled in microtubes at necropsy and forwarded to SARS-CoV-2 molecular examination. The protocol involved viral RNA extraction using a commercially available kit (MagMAX^{TM} Viral/Pathogen Nucleic Acid Isolation Kit, Applied Biosystems, Foster City, CA, USA) and detected by real-time polymerase chain reaction (RT-PCR) using a commercial kit (One/StepCOVID-19-IBMP kit, Instituto de Biologia Molecular do Paraná, Curitiba, PR, Brazil), that targets the N gene and ORF-1ab of SARS-CoV-2. The viral load was indicated as the cycle threshold (Ct) value of the SARS-CoV-2 N gene and ORF1ab. According to the manufacturer's protocol, Ct values of < 40 to the N gene and ORF1ab were positive for SARS-CoV-2 RNA.

Viral RNA was detected in the rectal swab, spleen and kidney. In this case, the diagnosis of natural SARS-CoV-2 infection was based on SARS-CoV-2 RNA molecular detection and nucleocapsid and spike tissue antigen detection. The Ct values of each SARS-CoV-2 target gene are summarized in Table 1. Many RT-qPCR assays use a Ct cut-off of 40 to indicate a positive result and detect a low number of RNA molecules (Tom and Mina, 2020), as seen in this case. Due to the high Ct values, we don't be able to sequence and identify the viral strain. As previously described in farmed-mink (*Neovison vison*), naturally infected by SARS-CoV-2 (Ritter et al. 2022), we observed patchy viral distribution in tissues. The absence of viral detection in the giant-anteater lungs by RT-qPCR, despite the nucleocapsid and spike immunolabeling, probably could be attributed to the sampling site. Due to this fact, we suggest the association of RT-qPCR and immunohistochemistry to increase the chances of SARS-CoV-2 diagnosis in wild animals.

SARS-CoV-2 infections in animals typically lead to an asymptomatic course (Jemerši´c et al. 2021). Although mild gross and microscopic pulmonary changes, no clinical respiratory signs were observed in this *M. tridactyla* with SARS-CoV-2 natural infection. This fact increases the need for environmental surveillance of the SARS-CoV-2 in potentially vulnerable hosts to infection, even in cases without evident clinical signs. Detecting animal SARS-

Table 1. SARS-COV-2 RT-PCR Cycle Threshold (Ct) Results in Different Tissues in a Naturally Infected Giant Anteater (*Myrmecophaga Tridactyla*).

	Target gene	
	N[1]	*ORF1ab*[1]
Nasal swab	ND	ND
Rectal swab	36.7	35.2
Lung	ND	ND
Spleen	36.8	37.23
Liver	ND	ND
Kidney	37.5	36.2

[1]Positive Ct cut-off value < 40; *ND* not detected.

CoV-2 reservoirs will help prevent and mitigate the spread of the virus into susceptible populations and is crucial to the One Health approach.

This report is the first evidence of natural SARS-CoV-2 infection in a Pilosa order species and shows a novel, susceptible host. The uncontrollable spread of human SARS-CoV-2 increases the need for surveillance to identify the potential host animals. The early detection of animal SARS-CoV-2 reservoirs will help prevent and mitigate the spread of the virus into susceptible populations and is crucial to one health maintenance.

Acknowledgments

We are thankfull to the Conselho Nacional de Desenvolvimento Científico e Tecnológico (CNPq), and Coordenação de Aperfeiçoamento de Pessoal de Nível Superior (CAPES) for the support of our study.

Data Availability

The data that support the findings of this study are available on request from the corresponding author.

Declarations

Conflict of interest The authors report no conflicts of interest.

References

Anderson RC, Chabaud AG, Wilmott S (2009) *Keys to the nematode parasites of vertebrates: archival volumes*, Cambridge: Cabi

Damas J, Hughes GM, Keough KC, Painter CA, Persky NS, Corbo M, et al. (2020) Broad host range of SARS-CoV-2 predicted by comparative and structural analysis of ACE2 in vertebrates. *Proceedings of the National Academy of Sciences* 117:22311–22322. https://doi.org/10.1073/pnas.2010146117

Jarrah SA, Kmetiuk LB, Carvalho OV, Sousa AT, Souza VR, Nakazato L, et al. (2022) Persistent SARS-CoV-2 antigen presence in multiple organs of a naturally infected cat from Brazil. *Journal of Venomous Animals and Toxins including Tropical Diseases* 28:e20210074. https://doi.org/10.1590/1678-9199-JVATITD-2021-0074

Jemeršić cL, Lojkić cI, Krešić cN, Keros T, Zelenika TA, Jurinović Cl, et al. (2021) Investigating the presence of SARS CoV-2 in free-living and captive animals. *Pathogens* 10:635. https://doi.org/10.3390/pathogens10060635

Johnston SC, Ricks KM, Jay A, Raymond JL, Rossi F, Zeng X, et al. (2021) Development of a coronavirus disease 2019 nonhuman primate model using airborne exposure. *PLoS One* 16:e0246366. https://doi.org/10.1371/journal.pone.0246366

Lean FZX, Núñez A, Spiro S, Priestnall SL, Vreman S, Bailey D, et al. (2021) Differential susceptibility of SARS-CoV-2 in animals: Evidence of ACE2 host receptor distribution in companion animals, livestock and wildlife by immunohistochemical characterization. *Transboundary and Emerging* 69:2275–2286. https://doi.org/10.1111/tbed.14232

Miranda F, Bertassoni A, Abba AM (2014) *Myrmecophaga tridactyla*. *The IUCN Red List of Threatened Species* 2014. Available: https://www.iucnredlist.org/fr/species/14224/47441961. [Accessed March 4th, 2022]. doi: https://doi.org/10.2305/IUCN.UK.2014-1.RLTS.T14224A47441961.

Munster VJ, Feldmann F, Williamson BN, van Doremalen N, Pérez-Pérez L, Schulz J, et al. (2020) Respiratory disease in rhesus macaques inoculated with SARS-CoV-2. *Nature* 585:268–272. https://doi.org/10.1038/s41586-020-2324-7

Ortlepp MA (1922) The Nematode genus *Physaloptera rudolphi*, 1819. *Proceedings of the Zoological Society of London* 2:999–1107

Pereira AH, Vasconcelos AL, Silva VL, Nogueira BS, Silva AC, Pacheco RC, et al. (2022) Natural SARS-CoV-2 infection in a free-ranging black-tailed marmoset (*Mico melanurus*) from an Urban Area in Mid-West Brazil. *Journal of Comparative Pathology* 194:22–27. https://doi.org/10.1016/j.jcpa.2022.03.005

Ritter JM, Wilson TM, Gary JM, Seixas JN, Martines RB, Bhatnagar J, et al. (2022) Histopathology and localization of SARS-CoV-2 and its host cell entry receptor ACE2 in tissues from naturally infected US-farmed mink (Neovison vison). *Veterinary Pathology* 59:681–695. https://doi.org/10.1177/03009858221079665

Tom MR, Mina MJ (2020) To interpret the SARS-CoV-2 test, consider the cycle threshold value. *Clinical Infectious Diseases* 71:2252–2254. https://doi.org/10.1093/cid/ciaa619

Vicente JJ, Rodrigues HO, Gomes DC, Pinto RM (1997) Nematoides do Brasil. Parte V: Nematoides de mamíferos. *Revista Brasileira De Zoologia* 14:1–452. https://doi.org/10.1590/S0101-81751997000500001